Electronic Supplementary Information (ESI)

Probing ultrafast dynamics during and after passing through conical intersections

Shunsuke Adachi[†], *Tom Schatteburg*[‡], *Alexander Humeniuk*[§], *Roland Mitric*[§], *Toshinori Suzuki*[†,*]

[†] Department of Chemistry, Graduate School of Science, Kyoto University, Kitashirakawa Oiwakecho, Sakyo-ku, Kyoto 606-8502, Japan

[‡] Laboratorium für Physikalische Chemie, ETH Zürich, 8093 Zürich, Switzerland

[§] Institut für physikalische und theoretische Chemie, Julius-Maximilians-Universität Würzburg, Emil-Fischer-Str. 42, D-97074 Würzburg, Germany

Corresponding Author: suzuki@kuchem.kyoto-u.ac.jp

Entire TRPES spectra. Figure S1(a) and (b) show two different eBE regions of the same TRPES spectra measured as a function of delay time between the pump and the probe pulses. The static photoelectron spectrum of furan (Fig. S1(c)) was measured using the 14-eV source in our laboratory.

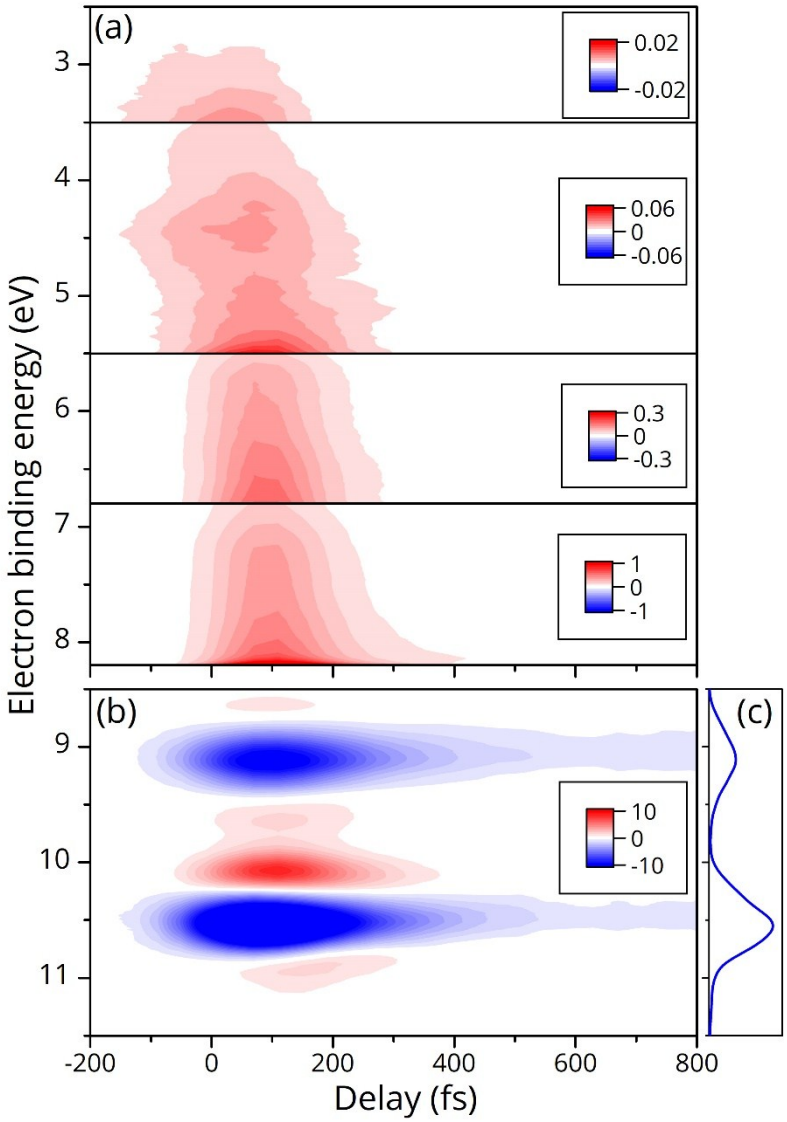

Figure S1. TRPES spectra in (a) lower and (b) higher eBE regions. (c) Static photoelectron spectrum of furan.

Lower- and upper-state potential energy surfaces. eBE depends not only on a lower (i.e. neutral) state potential energy surface, but on difference between lower and upper (i.e. cationic) state PESs. Furan has a planar equilibrium geometry both in the neutral ground state S_0 and in the cation ground state D_0. For S_0 this can be explained by aromaticity, while for D_0 this is proven by geometry optimization at the DFT level of theory. The harmonic frequencies are all positive confirming that the planar geometry is indeed a minimum. The puckering of the oxygen out of the molecular plane therefore raises the energies of both S_0 and D_0. As the conical intersection is approached, the potential energy surfaces of S_0 and D_0 move in parallel and go up steeply. On the other hand the energy of the S_1 state decreases until the S_1 and S_0 states cross at the conical intersection. Based on this reasoning we can qualitatively draw the energies of S_0, S_1 and D_0 along the reaction coordinate in Fig. S2. Clearly the vertical ionization energy from the current electronic state to D_0 increases (orange arrows in the sketch). In our trajectory-based simulations we observed exactly this predicted behavior as can be seen in Fig. 2b of our previous publication[1]. Accordingly, in TRPES, motion toward CIs on the excited-state surfaces are observed as a gradual spectral shift toward higher eBE[2,3].

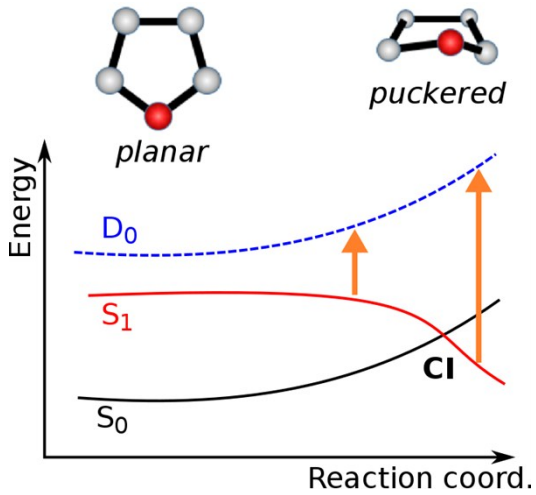

Figure S2. Qualitative sketch S_0, S_1 and D_0 state energies along the reaction coordinate connecting the ground state minimum and the puckered conical intersection geometries.

Contribution of cationic excited states in the simulated TRPES spectra. In the simulated TRPES spectra (Fig. 2(b)), we have only taken account of the cation ground state (D_0) when computing vertical ionization energies, although the cationic excited states (D_n) are also energetically accessible (see Fig. S3). This can be rationalized by Koopmans' correlation; the $D_0(\pi^{-1})$ state is dominant when photoionization occurs from the $^1B_2(\pi\pi^*)$ excited state [Arrow (i) in Fig. S3]. On the other hand, photoionization to the D_n states as well to the D_0 state can contribute to the photoelectron signals when photoionization occurs after returning to the ground state [Arrow (ii)]. The contributions of the cationic excited states leads to spectral broadening toward higher eBE[4]. However, it appears the feature associated with the nonadiabatic transition (i.e. the kink) in the TRPES spectra remains preserved[4].

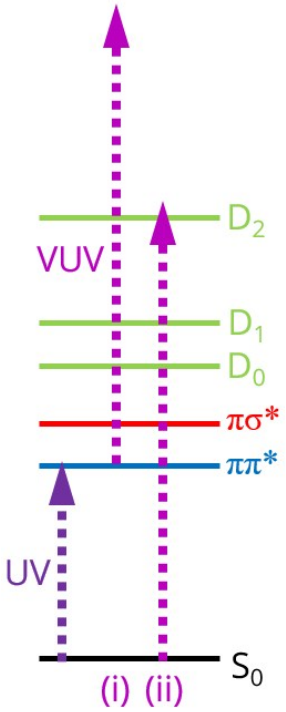

Figure S3. Energy level diagram of furan.

Spectral intensity calibration using He(I) reference spectrum. The transmission efficiency of our apparatus drops largely for low-energy photoelectrons (PKE < 0.5 eV). In addition, the efficiency also gradually declines for high-energy photoelectrons. It appears that high-energy photoelectrons hit the entrance skimmer and/or solenoid tube of our magnetic-bottle photoelectron spectrometer and are unable to reach the detector. Figure S4(a) shows the static photoelectron spectrum of furan measured in our laboratory (identical with Fig. S1(c)). The relative intensities of the two bands (~9.1 and ~10.5 eV) differ from those of a He(I) reference spectrum[5] (dashed curve in Fig. S4(b)) by a factor of around three. This difference may be attributed to the non-uniform transmission efficiency of our magnetic-bottle photoelectron spectrometer. For furan, relative photoionization cross sections of the first two bands stay similar for photon energies from 15 to 25 eV[6]. Assuming that this trend also applies for 14 eV, intensity calibration to match the He(I) reference spectrum was performed (solid curve in Fig. S4(b)). Since there exist only two peaks in the displayed region, a linear function was used as a scaling model.

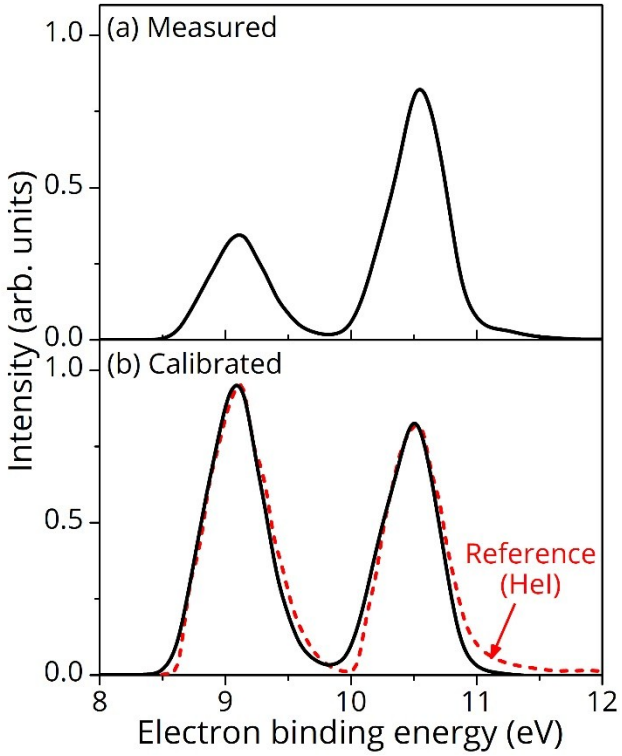

Figure S4. (a) Static photoelectron spectrum of furan measured using the 14-eV source in our laboratory. (b) Calibrated (solid) and He(I) reference (dashed) spectra.

Experimental and calculated vertical ionization energies of furan and 1,3-butadienal. Figure S4 shows experimental and calculated vertical ionization energies of furan and 1,3-butadienal (a ring-opened isomer of furan). The static photoelectron spectrum of furan is shown in Fig. S1(c). That of 1,3-butadienal was reported by Mohmand *et al*.[7], in which there exist two bands (~8.7 and ~11.3 eV) in the displayed eBE region in Fig. S5. These experimental vertical ionization energies could be reproduced within 0.3 eV in our calculations.

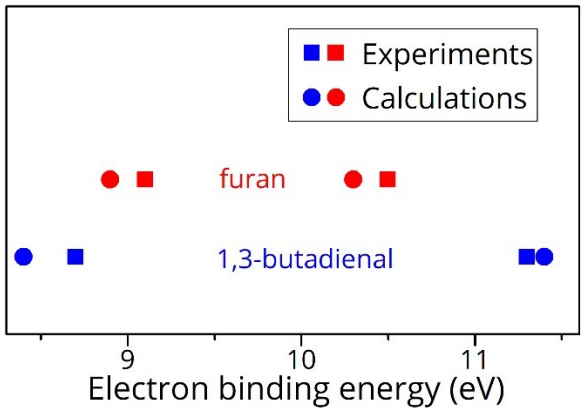

Figure S5. Experimental and calculated vertical ionization energies of furan and 1,3-butadienal.

Subsequent ground-state reactions after passing through the puckering CI. We argued that vibrationally excited furan is predominantly formed by nonadiabatic transition to the ground state, and that subsequent reactions proceed in the ground state at later time[2]. Fig. S6 shows a snapshot of intermediate photoproducts at τ = 2 ps as a consequence of the ground-state reactions obtained by the TDDFT simulations. The by far largest portion of trajectories (~94%) remains in the region of furan and the related oxabicyclopentene; in the furan molecule after passing through the puckering CI, the oxygen swings back and forth wildly, taking the geometry from oxabicyclopentene to planar furan and back to oxabicyclopentene with the oxygen on the other side of the ring. Therefore, it is not easy to discriminate trajectories found as furan and oxabicyclopentene in the vibrationally excited states, and there exists substantially large uncertainty in the simulated QY of oxabicyclopentene (η = 0.00 ~ 0.23). Meanwhile, they could also turn into cyclopropne-carbaldehyde (η ~ 0.03), when the valencies on the carbon atoms are saturated by forming a cyclopropene ring. Accordingly, the simulated total photoproduct QY is η = 0.04 ~ 0.3. This appears qualitatively consistent with the experimental one (η = 0.09).

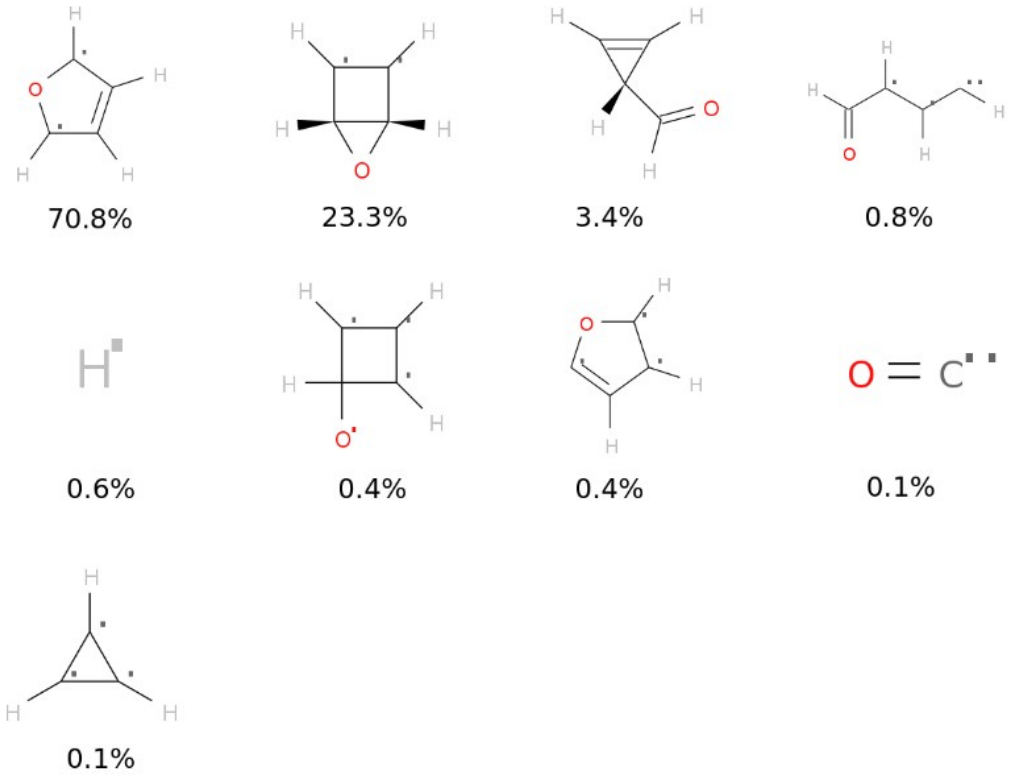

Figure S6. Snapshot of optimized photoproducts after 2 ps sorted by their abundance.

1 A. Humeniuk, M. Wohlgemuth, T. Suzuki and R. Mitrić, Time-resolved photoelectron imaging spectra from non-adiabatic molecular dynamics simulations, *J. Chem. Phys.*, 2013, **139**, 134104.

2 T. Fuji, Y.-I. Suzuki, T. Horio, T. Suzuki, R. Mitrić, U. Werner and V. Bonačić-Koutecký, Ultrafast photodynamics of furan, *J. Chem. Phys.*, 2010, **133**, 234303.

3 S. P. Neville, Y. Wang, A. E. Boguslavskiy, A. Stolow and M. S. Schuurman, Substituent effects on dynamics at conical intersections: Allene and methyl allenes, *J. Chem. Phys.*, 2016, **144**, 014305.

4 R. Mitrić, U. Werner and V. Bonačić-Koutecký, Nonadiabatic dynamics and simulation of time resolved photoelectron spectra within time-dependent density functional theory: Ultrafast photoswitching in benzylideneaniline, *J. Chem. Phys.*, 2008, **129**, 164118.

5 K. Kimura, S. Katsumata, Y. Achiba, T. Yamazaki and S. Iwata, *Handbook of HeI Photoelectron Spectra of Fundamental Organic Compounds*, Japan Scientific Soc. Press, Tokyo, 1981.

6 A. Ponzi, M. Sapunar, C. Angeli, R. Cimiraglia, N. Došlić and P. Decleva, Photoionization of furan from the ground and excited electronic states, *J. Chem. Phys.*, 2016, **144**, 084307.

7 S. Mohmand, T. Hirabayashi and H. Bock, Gasphasen-Reaktionen, 22. Thermische Erzeugung von C4H4O: Vinylketen und Ethylidenketen, *Chem. Ber.*, 1981, **114**, 2609–2621.